



OPEN

Small tRNA-derived RNAs are increased and more abundant than microRNAs in chronic hepatitis B and C

SUBJECT AREAS:
HEPATITIS B VIRUS
HEPATITIS C VIRUS
TRANSCRIPTOMICS
CANCER GENOMICS

Sara R. Selitsky^{1,2,3,4}, Jeanette Baran-Gale^{1,2}, Masao Honda⁵, Daisuke Yamane^{3,4}, Takahiro Masaki^{3,4}, Emily E. Fannin², Bernadette Guerra⁶, Takayoshi Shirasaki⁵, Tetsuro Shimakami⁵, Shuichi Kaneko⁵, Robert E. Lanford⁶, Stanley M. Lemon^{3,4*} & Praveen Sethupathy^{1,2,4*}

Received
8 August 2014

Accepted
5 December 2014

Published
8 January 2015

¹Bioinformatics and Computational Biology Curriculum, University of North Carolina at Chapel Hill, Chapel Hill, North Carolina, United States of America, ²Department of Genetics, University of North Carolina at Chapel Hill, Chapel Hill, North Carolina, United States of America, ³Departments of Medicine and Microbiology & Immunology, University of North Carolina at Chapel Hill, Chapel Hill, North Carolina, United States of America, ⁴Lineberger Comprehensive Cancer Center, University of North Carolina at Chapel Hill, Chapel Hill, North Carolina, United States of America, ⁵Department of Gastroenterology, Kanazawa University Graduate School of Medicine, Kanazawa, Japan, ⁶Department of Virology and Immunology, Texas Biomedical Research Institute and Southwest National Primate Research Center, San Antonio, Texas, United States of America.

Correspondence and requests for materials should be addressed to P.S. (praveen_sethupathy@med.unc.edu)

* These authors contributed equally to this work

Persistent infections with hepatitis B virus (HBV) or hepatitis C virus (HCV) account for the majority of cases of hepatic cirrhosis and hepatocellular carcinoma (HCC) worldwide. Small, non-coding RNAs play important roles in virus-host interactions. We used high throughput sequencing to conduct an unbiased profiling of small (14–40 nts) RNAs in liver from Japanese subjects with advanced hepatitis B or C and hepatocellular carcinoma (HCC). Small RNAs derived from tRNAs, specifically 30–35 nucleotide-long 5' tRNA-halves (5' tRHs), were abundant in non-malignant liver and significantly increased in humans and chimpanzees with chronic viral hepatitis. 5' tRH abundance exceeded microRNA abundance in most infected non-cancerous tissues. In contrast, in matched cancer tissue, 5' tRH abundance was reduced, and relative abundance of individual 5' tRHs was altered. In hepatitis B-associated HCC, 5' tRH abundance correlated with expression of the tRNA-cleaving ribonuclease, angiogenin. These results demonstrate that tRHs are the most abundant small RNAs in chronically infected liver and that their abundance is altered in liver cancer.

Hepatitis B virus (HBV) and hepatitis C virus (HCV) are phylogenetically unrelated non-cytopathic viruses that infect the liver¹. While HBV is a DNA virus, and HCV is a positive-strand RNA virus, both have the capacity to persist for years in some infected individuals. Hundreds of millions of people worldwide are chronic carriers of HBV or HCV, 30–50% of whom have chronic liver disease². Together, these viral infections are responsible for ~60% of liver cirrhosis and ~80% of hepatocellular carcinoma (HCC), a leading cause of cancer-related deaths worldwide. Numerous studies suggest that microRNAs (miRNAs), small 21–23 nt non-coding RNAs are important in the pathogenesis of these infections, modulating viral replication as well as host responses and possibly influencing the risk of carcinogenesis³. For example the HBV X protein represses expression of miR-148a, potentially enhancing tumorigenesis⁴. In contrast, HCV infection is associated with higher expression of miR-21, which targets key components of Toll-like receptor signaling pathways, possibly facilitating viral evasion of innate immune responses⁵. miR-122 stabilizes HCV RNA and promotes its replication^{6,7}, and the importance of this interaction is reflected in the clinical development of an anti-miR-122 antagomir (miravirsin) as an antiviral therapeutic⁸.

Somewhat larger, 30–35 nt RNAs derived from the 5' half of tRNA (5' tRHs) represent a second major class of small non-coding RNA⁹. Increased expression of 5' tRHs has been associated with viral and rickettsial infections in animals^{10,11}, and may serve to prevent apoptosis and promote cell survival¹². However, they have not been studied previously in the context of viral hepatitis. To our knowledge, only one study has described unbiased profiling of small RNAs in the liver during chronic viral hepatitis¹³, but the analysis was restricted to miRNAs. We sequenced small (14–40 nts) RNAs in liver biopsies from subjects with chronic hepatitis and HCC, examining both non-tumor and matched cancer tissue, and found a surprisingly high proportion of reads representing 5' tRHs⁹. Our results document their presence in human tissue, demonstrate that they are the most highly abundant

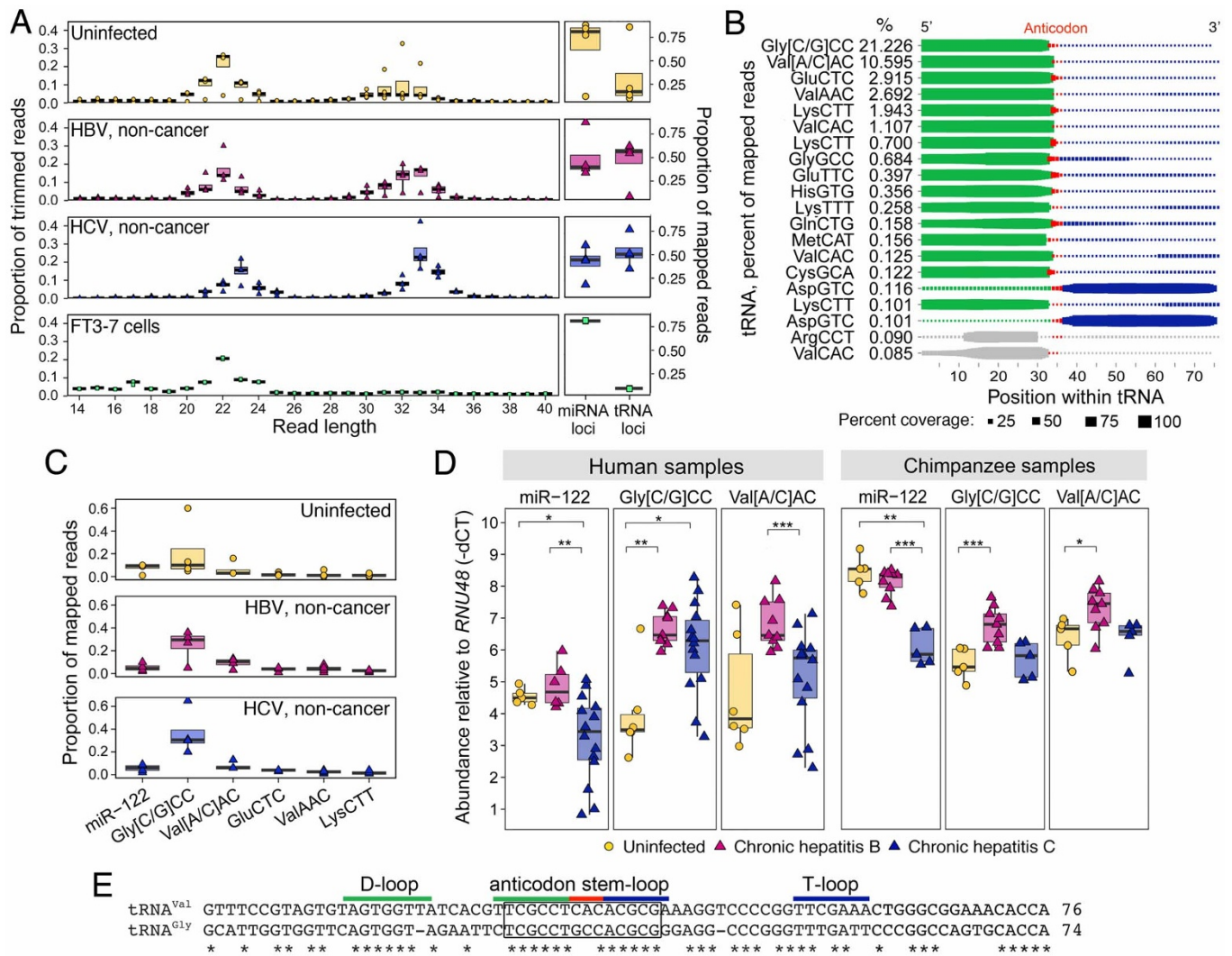


Figure 1 | tRH abundance in HBV- and HCV-infected liver. (a) (left) Read length distribution of 14–40 nt RNAs in non-malignant liver from uninfected, HBV-, or HCV-infected subjects ($n=4$ each), and FT3-7 cells ($n=3$ replicates). (right) Proportion of reads mapping to miRNA versus tRNA loci. Boxes represent median $\pm 1.5 \times$ interquartile range. (b) tRNA coverage plot from the average of the 20 non-cancer samples. Dot size represents percent of reads mapping at each base position within each tRNA (top 20 by average abundance). The anticodon is red, with 5' bases green and 3' bases blue. Gray: bases of RNAs that are non-tRNAs. See Supplemental Figure 1. (c) Proportion of mapped reads aligning to miR-122 versus the five most abundant tRNA-derived RNAs. (d) (left) Expression levels (RT-qPCR) of miR-122, 5' tRH^{Gly} ("Gly[C/G]CC") and 5' tRH^{Val} ("Val[A/C]AC") in uninfected ($n=5-6$), HBV-infected ($n=6-9$) and HCV-infected ($n=14$) human liver. Numbers of samples differ due to limited RNA. (right) Similar results from uninfected ($n=5$), HBV-infected ($n=9$), and HCV-infected C ($n=5$) chimpanzees. *RNU48* was used as a normalizer. * $P < 0.05$; ** $P < 0.01$; *** $P < 0.005$ by Mann-Whitney *U*-test. (e) ClustalW⁴³ multiple sequence alignment of representative tRNA^{Gly} and tRNA^{Val} genes from which 5' tRH^{Gly} and 5' tRH^{Val} could originate (see Supplemental Figure 3). tRNAs regions are highlighted according to the color scheme in panel (b). The box identifies a unique conserved sequence motif described in the text. "Mapped reads" represents all reads aligning to miRNAs or tRNAs (see Methods).

small RNAs in virus-infected liver, and show that their abundance is altered in various disease states including hepatocellular carcinoma.

Results

tRNA-half abundance is significantly increased in chronic viral hepatitis.

We employed high-throughput sequencing to characterize the small RNA transcriptome in liver tissue from Japanese adults with advanced hepatitis B or hepatitis C and concomitant HCC (see Supplemental Table 1 for patient information; see Supplemental Tables 2–4 for summary statistics on RNA, qRT-PCR, and sequencing). Initial studies focused on non-malignant tissue from 4 subjects with hepatitis B (mean age 53 ± 4 yrs s.e.m.), 4 with hepatitis C (63 ± 2 yrs), and 4 uninfected individuals undergoing resection of metastatic tumors (60 ± 10 yrs)¹⁴. A large proportion of the sequencing reads were 19–25 nts in length (median 38%, range 10–73%), as expected for miRNAs¹⁵ (Figure 1a, left). However, we

detected an equal or greater abundance of 30–35 nt reads in HBV- and HCV-infected liver (median 54%, range 14–80%). These larger RNAs were less abundant in uninfected tissue (median 21%, range 14–84%) and in human hepatoma (FT3-7) cells (median 9%, range 8.7–9.3%).

Most (~65%) of the 30–35 nt reads in infected samples aligned perfectly to the region 5' of the anticodon triplet in annotated tRNA genes¹⁶ (Figure 1b, Supplemental Figure 1, Supplemental Table 5 and 6). We refer to these as "5' tRNA-halves" (5' tRHs)⁹. Many of the remaining 30–35 nt reads also aligned to the 5' end of tRNAs, particularly tRNA^{Gly}, but with one or more nucleotide deletions. Also present were 3' tRHs (~36–39 nts) mapping to the region 3' of the anticodon, including the 3' terminal CCA (Figure 1b, Supplemental Figure 1). Additionally, we identified shorter reads derived from 3' or 5' tRNA termini, referred to previously as "tRNA fragments"⁹ (tRFs), or the region immediately 5' or 3' of the anticodon loop, but these



were much less frequent. In 6 of 8 infected livers, more reads mapped to tRNA loci¹⁶ than to known miRNAs¹⁷ (see Methods), while the opposite was true in 3 of 4 uninfected tissues as well as FT3-7 cells (Figure 1a, right).

There are 625 annotated tRNA genes in the human genome (hg19) encoding 458 unique tRNA sequences. We identified reads mapping to 348 of these 458 sequences. Notably, in 11 of the 12 subjects, the same five 5' tRHs comprised >80% of tRNA-derived reads (Supplemental Figure 2a). The two most abundant 5' tRHs were Gly[C/G]CC ("5' tRH^{Gly}"), which could be derived from any of 10 tRNA^{Gly} genes with identical 5' sequence, and Val[A/C]AC ("5' tRH^{Val}"), which could originate from any of 15 tRNA^{Val} genes (Figure 1b and c, Supplemental Figure 1 and 3, and Supplemental Table 5)¹⁶. 5' tRH^{Gly} accounted for 54 ± 9% (s.d.) and 5' tRH^{Val} 17 ± 9% of all tRNA-derived RNA reads (Supplemental Figure 2a). Remarkably, 5' tRH^{Gly} abundance exceeded that of miR-122, one of the most abundant liver miRNAs¹³, in 7 of 8 virus-infected tissues.

We used real-time reverse transcription quantitative PCR (RT-qPCR) to validate these results and compare 5' tRH^{Gly}, 5' tRH^{Val} and miR-122 abundance in liver tissue from 22 additional subjects (Supplemental Table 1–3)¹⁴. These analyses confirmed that 5' tRH^{Gly} abundance was increased in HBV- and HCV-infected liver compared with uninfected tissues ($P < 0.01$ and $P < 0.05$, respectively) (Figure 1d, left). A similar trend was observed for 5' tRH^{Val} (HBV $P = 0.07$; HCV $P = 0.7$). 5' tRH^{Gly} and 5' tRH^{Val} were more abundant than miR-122 in HBV- and HCV-infected liver (5' tRH^{Gly}, $P < 0.005$ for both HBV and HCV; 5' tRH^{Val}, $P < 0.005$ for HBV and $P < 0.01$ for HCV) (Figure 1d left). Notably, 5' tRH^{Val} abundance was higher in HBV- than in HCV-infected tissues ($P < 0.005$).

Chimpanzees (*Pan troglodytes*) recapitulate many aspects of HBV and HCV infections in humans^{18,19}, and are free of potential confounding variables (e.g., alcohol intake, smoking) that are difficult to control in human cohorts. Similar to humans, we found that intrahepatic 5' tRH^{Gly} and 5' tRH^{Val} abundance was increased in archived liver tissue from chimpanzees chronically infected with HBV compared to uninfected animals ($P < 0.005$ and $P < 0.05$, respectively) (Figure 1d, right, and Supplemental Table 7). However, 5' tRH abundance was not increased in chronically HCV-infected chimpanzee liver.

In human tissues, the relative abundance of specific tRNA-derived RNAs correlated with codon usage (codon frequency in DNA sequence) (Spearman's $\rho = 0.32$, $P = 0.01$) and the number of possible tRNA genes from which each could originate ($\rho = 0.41$, $P = 0.001$) (Supplemental Figure 2b). However, tRNAs representing potential sources of the five most abundant tRHs were not the most highly ranked by gene number or codon usage, suggesting that additional factors likely determine tRH biogenesis (Supplemental Figure 4). Interestingly, those tRNAs from which 5' tRH^{Gly} and 5' tRH^{Val} are potentially derived share a unique sequence motif in the anticodon stem-loop region (Figure 1e) not present in other tRNAs (Supplemental Figure 3).

tRNA-half abundance is altered in viral hepatitis associated cancer. In HCC tissue from HBV-infected subjects, RT-qPCR analysis showed that 5' tRH^{Gly} and 5' tRH^{Val} abundance was significantly reduced ($P < 0.005$ for both) (Figure 2a). Similar reductions were evident in HCV-associated cancer tissue, but significant only for 5' tRH^{Val} ($P < 0.05$). We then sequenced small RNAs in cancer tissue from 4 HBV- and 4 HCV-infected subjects. The proportion of reads mapping to tRNA genes was reduced in 4 of 7 samples for which a paired analysis with non-malignant liver was possible, and relatively unchanged in the other 3 (Figure 2b). Although tRNA-derived RNA expression profiles were similar across non-malignant tissues from different subjects, there was substantial variation when compared to cancer tissues (Figure 2c). This suggests that the relative abundance of specific tRNA-derived

RNAs is altered in HCC. Notably, the relative abundance of 5' tRH^{Gly} was reduced by ~50–60% in both HBV- and HCV-associated cancer (Figure 2d).

tRNA-half abundance correlates with angiogenin levels in HBV-associated cancer. Angiogenin (encoded by the gene *ANG*) is best known for its role in angiogenesis, but several studies suggest its RNase activity contributes to tRH biogenesis^{20,21}. Consistent with this, analysis of previous microarray data obtained from these tissues¹⁴ revealed that *ANG* mRNA was reduced in both HBV- and HCV-associated cancer compared to non-malignant tissue ($P < 0.01$ and $P < 0.005$, respectively) or uninfected liver ($P < 0.005$ and $P = 0.01$) (Figure 3a). Analysis of data from The Cancer Genome Atlas (<https://tcga-data.nci.nih.gov/tcga/>) also indicates that *ANG* expression is reduced in HCC compared to non-malignant tissue, although the difference is significant only for HBV-associated cancer (HBV $P < 0.005$, HCV $P = 0.12$) (Supplemental Figure 5). *ANG* mRNA abundance correlated strongly with 5' tRH expression in the HBV-infected subjects we studied (5' tRH^{Gly}: Spearman's $\rho = 0.67$, $P < 0.01$; 5' tRH^{Val}: $\rho = 0.74$, $P < 0.005$) (Figure 3b). Quantitative immunoblot analyses (Supplemental Figure 6) confirmed a correlation between *ANG* protein abundance and 5' tRH expression in HBV-associated cancer (5' tRH^{Gly}: $\rho = 0.83$, $P < 0.005$; 5' tRH^{Val}: $\rho = 0.87$, $P < 0.005$) (Figure 3c). *ANG* was expressed within the cytoplasm of hepatocytes (Figure 3d), and although its expression varied substantially in different tumors (Figure 3e), reductions in *ANG* expression likely explain the reduced tRH abundance we observed in most HBV-associated cancers. Unfortunately, however, the available tissue sections from these subjects were insufficient to power a formal analysis of the correlation between cytoplasmic versus nuclear expression of *ANG* and tRH abundance. *ANG* expression correlated poorly with tRH abundance in HCV-infected livers, suggesting that other factors determine tRH biogenesis.

Discussion

Recent advances in high-throughput sequencing technology have unveiled the complexity and diversity of functional small RNAs. We found that small RNAs derived from tRNAs, specifically 5' tRNA-halves⁹ (5' tRHs, ~30–35 nts), are abundant in liver, significantly increased during chronic viral infection, and altered in abundance in liver cancer associated with these infections. We do not believe that these tRNA-halves are products of stochastic endonuclease cleavage of tRNAs for several reasons. First, the same tRNA-halves were found to be increased in chronic viral hepatitis across all individuals. Second, each tRNA-half family exhibited a uniform length distribution (e.g., 5' tRH^{Gly} was represented primarily by reads of length 32–34 in every individual). Third, tRNA-halves were preferentially induced in chronic HBV infection (as compared to chronic HCV infection) in both human and chimpanzee tissue, indicating biological specificity. Finally, tRH abundance was correlated with disease state (cancer versus non-cancer), indicating reproducible sensitivity to the cellular environment.

Several models of disease have been shown to exhibit an increase in tRH abundance, including cultured human airway cells infected with respiratory syncytial virus²², mice infected with spotted-fever group rickettsia²³, and rats treated with cisplatin²⁴. While their function is not well understood, previous work in cell culture suggests that some tRHs promote cell survival, are anti-apoptotic¹², reduce translation²⁵, and promote the formation of stress granules²⁶. Preliminary studies in our laboratory do not support a role for 5' tRH^{Gly} or 5' tRH^{Val} in the regulation of global protein translation in human hepatoma cells (Supplemental Figure 7–8); however, more detailed investigation is required to uncover the potential functions of tRHs. It has also been suggested that tRHs may alter the immune response due to their enrichment in mouse lymphoid organs²⁷, high

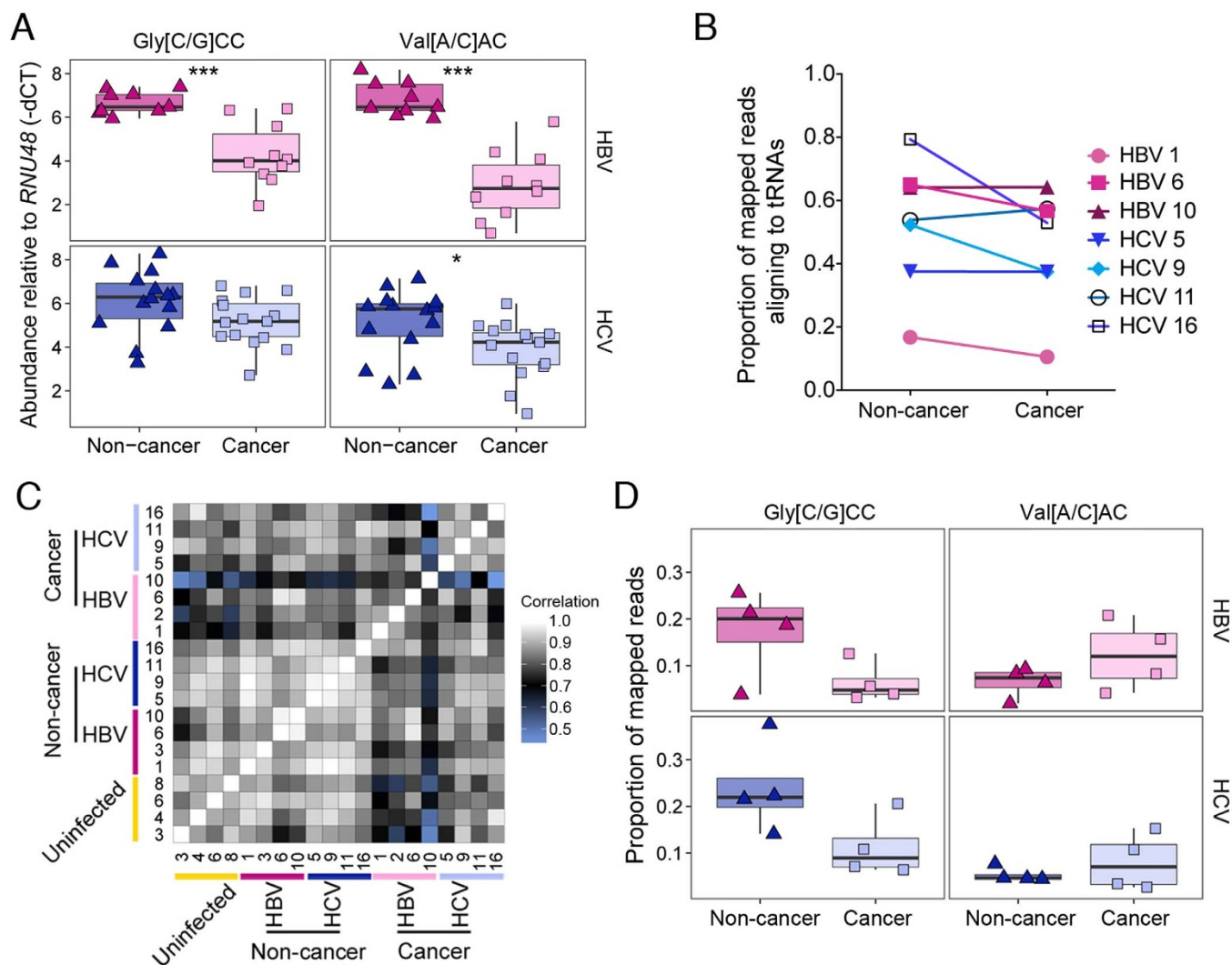


Figure 2 | 5' tRH abundance in HBV- and HCV-associated hepatocellular carcinoma. (a) Abundance (RT-qPCR) of (left) 5' tRH^{Gly} (Gly[C/G]CC) and (right) 5' tRH^{Val} (Val[A/C]AC) in (top) non-malignant ($n=9$) and cancer tissue ($n=10$) from HBV-infected subjects, and (bottom) non-malignant ($n=14$), and cancer tissue ($n=15$) from HCV-infected subjects. Box and whisker plots are overlaid with data from each sample; whiskers extend to 1.5 * interquartile range. P-values calculated using Mann-Whitney *U*-test. * $P < 0.05$; ** $P < 0.01$; *** $P < 0.005$. (b) Proportion of mapped reads aligning to tRNAs for the paired cancer and non-cancer tissue from subjects with chronic hepatitis B ($n=3$) and hepatitis C ($n=4$) (c) Correlation heatmap of tRNA-derived RNA expression profiles determined by small RNA sequencing. The colors of the cells represent Spearman's rank correlation coefficients of the relative levels of the 10 most abundant tRNA-derived RNAs between all pairs of tissue samples sequenced ($n=20$). (d) Proportion of mapped reads that align to 5' tRH^{Gly} and 5' tRH^{Val} in non-malignant and cancer tissue from (top) HBV-infected and (bottom) HCV-infected subjects. "Mapped reads" represents all reads aligning to miRNAs or tRNAs (see Methods).

abundance in seminal exosomes (considered to be immunosuppressive)²⁸, and roles in facilitating *Trypanosoma cruzi* infection in human cells and altering host gene expression²⁹.

There is good evidence that the abundance of these small non-coding RNAs increases in response to specific kinds of cellular stress. For example, tRHs are induced in cell culture by the addition of sodium arsenite, exposure to UV, nutrient starvation, hypoxia, hypothermia and heat, but not by exposure to etoposide, γ -radiation, caffeine^{30,31}. This strongly suggests that the formation of tRHs is a regulated process, rather than due to general degradation of tRNAs in response to stress. In the nucleus angiogenin is involved in promoting angiogenesis³² and in the cytoplasm, when not bound to RNH1, it acts as a tRNA-processing RNase^{33,34}, cleaving tRNAs at the anticodon loop and producing tRHs^{30,31}. The cellular localization of angiogenin and its ribonuclease activity depend on the intracellular conditions and are regulated by RNH1³³. The differences we observed in correlations between ANG expression and tRH abundance in chronic hepatitis B, hepatitis C and

associated liver cancer may be a result of differences in angiogenin localization and function in these disease states. Non-tumor and tumor tissues from patients with chronic hepatitis C tend to show more evidence of angiogenesis than the in chronic hepatitis B^{35,36}. This could mean that in chronic hepatitis C angiogenin is primarily nuclear, and therefore not exclusively involved in tRH production. Finally, it must also be noted that factors other than ANG may be critical to tRH biogenesis in different cell types or in response to different types of cellular stress. Much more remains to be uncovered about the specific mechanisms that lead to tRH accumulation.

Chronic infections with HBV and HCV typically lead to more severe liver disease in human patients than in the chimpanzee model^{37,38}. Disease severity may account for the differences we observed in tRH abundance between liver tissue from human subjects with chronic HCV infection and the chimpanzee samples. Interestingly, however, humans and chimpanzees exhibited similar increases in tRH abundance in chronic hepatitis B, suggesting that

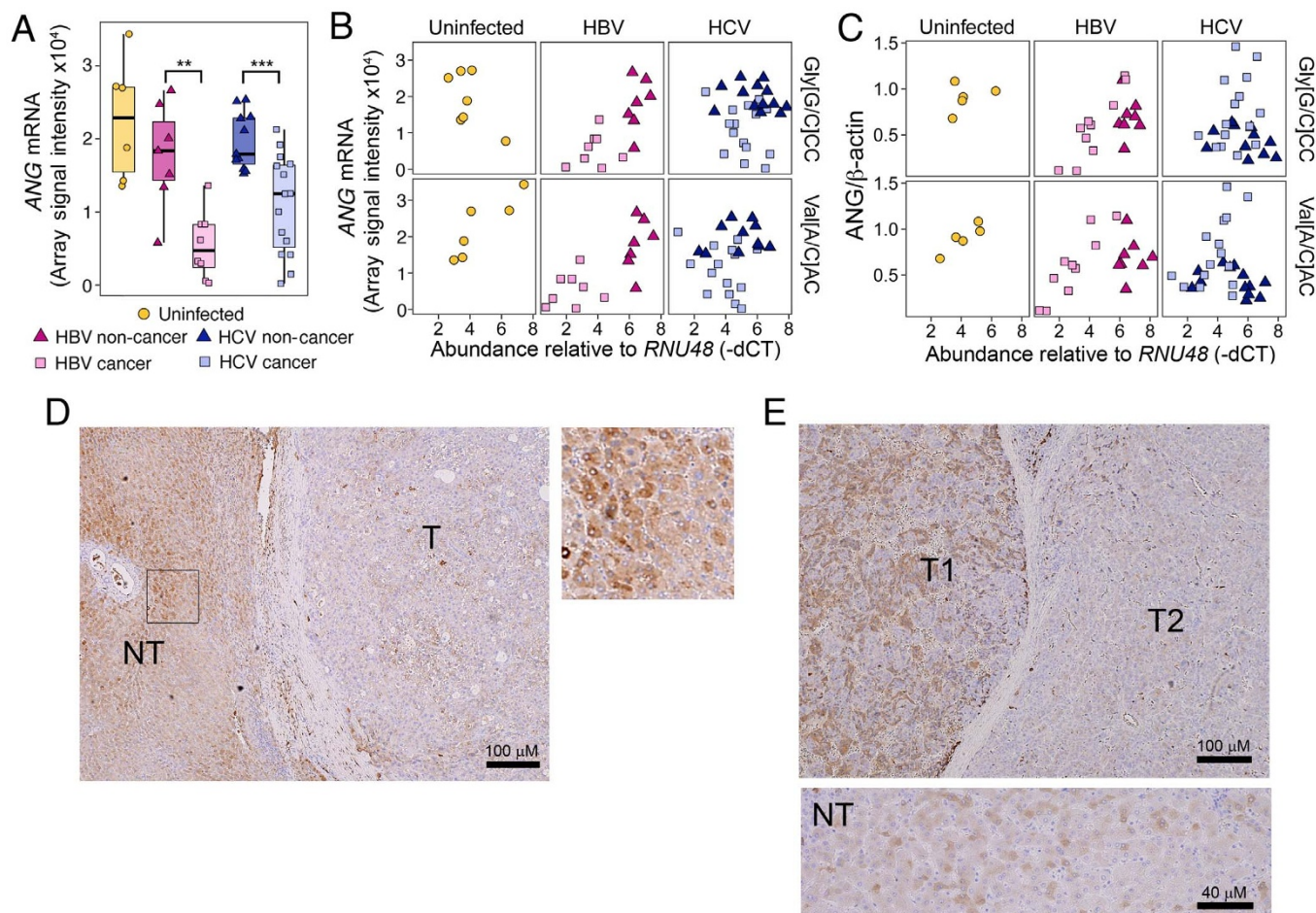


Figure 3 | Angiogenin expression in viral hepatitis and hepatocellular carcinoma. (a) Normalized ANG mRNA levels from previously generated liver microarray data¹⁴ from uninfected subjects ($n=6$), non-malignant ($n=7$) and liver cancer ($n=8$) tissue from HBV-infected subjects, and non-malignant ($n=11$) and cancer tissue ($n=15$) from HCV-infected subjects. ** $P < 0.01$; *** $P < 0.005$, calculated by Mann-Whitney *U*-test. (b) Scatter plot of the levels of 5' tRHs (RT-qPCR, -dCT normalized to *RNU48*) and ANG mRNA (microarray). 5' tRH^{Gly} ("Gly[C/G]CC"): uninfected subjects ($n=7$), non-cancer ($n=7$) and cancer ($n=8$) liver tissue from chronic hepatitis B subjects, and non-cancer ($n=11$) and cancer ($n=15$) liver tissue from chronic hepatitis C subjects; 5' tRH^{Val}: uninfected subjects ($n=6$), non-cancer ($n=7$) and cancer ($n=8$) liver tissue from chronic hepatitis B subjects, and non-cancer ($n=11$) and cancer ($n=15$) liver tissue of chronic hepatitis C subjects. (c) Scatter plot of the levels of 5' tRHs (RT-qPCR, -dCT normalized to *RNU48*) and ANG protein expression (normalized to β -actin) determined by immunoblot analysis. (d) Immunohistochemistry staining for ANG in formalin-fixed non-tumor (NT) and tumor tissue (T) from HBV-infected subject #10. (Right) Magnified view of non-tumor (NT). (e) ANG staining in adjacent tumor nodules (T1 and T2) and in non-tumor (NT) tissue from HCV-infected subject #7.

there may be a primary HBV-specific mechanism that directly regulates tRH biogenesis.

Our study has some technical limitations. tRNAs are subject to many different chemical modifications³⁹, several of which could impede library preparation and sequencing. This may have biased which tRNA-derived RNAs we detected. Also, we do not know how tRH abundance varies among the diverse cell types that populate the liver. Given that these small RNAs have not previously been studied in human tissue, we also have little appreciation of what functions these small non-coding RNAs have within the liver. Nonetheless, our finding that the intrahepatic abundance of tRHs is substantially increased in chronic viral infections of the liver and altered in HCC suggest that tRHs may have important, yet to be determined roles in liver disease. Thus, this study may have implications for disease pathogenesis and novel therapeutic strategies.

Methods

The methods were carried out in accordance with the approved guidelines.

Human subjects. Written informed consent was obtained from all human subjects. Ethics approval was obtained from the Ethics Committee for Human Genome/Genes Analysis Research at Kanazawa University Graduate School of Medical Science.

Chimpanzee liver tissue. The chimpanzee samples used in this study were archived from previous studies and were collected prior to December 15, 2011. Chimpanzees were housed and cared for at the Southwest National Primate Research Center (SNPRC) of the Texas Biomedical Research Institute. The animals were cared for in accordance with the Guide for the Care and Use of Laboratory Animals, and all protocols were approved by the Institutional Animal Care and Use Committee. SNPRC is accredited by the Association for Assessment and Accreditation of Laboratory Animal Care (AAALAC) International. SNPRC operates in accordance with the NIH and U.S. Department of Agriculture guidelines and the Animal Welfare Act. Animals were sedated for all procedures. Animals are group-housed with indoor and outdoor access and an environmental enrichment program is provided by a staff of behavioral scientists.

Small RNA-sequencing. RNA was isolated as described previously¹⁴. RNA purity was assessed with Nanodrop 2000 (Thermo Scientific) and integrity was determined with an Agilent 2100 Bioanalyzer (Agilent). RNA integrity and sequencing quality were comparable for all specimens (Supplemental Table 2–4). Small RNA libraries were generated using Illumina TruSeq Small RNA Sample Preparation Kit (Illumina, San Diego, CA). Sequencing was performed on Illumina HiSeq 2000 platform. Bioinformatic analysis: Sequencing reads were trimmed using Cutadapt (parameters $O -10 e 0.1$) and were further analyzed in two different ways: (i) Mapped trimmed reads allowing no mismatches to all tRNA sequences (except pseudo-tRNAs and undefined tRNAs) downloaded from GTRNAdb¹⁶ (Figure 1b,c; Figure 2c,d; Supplemental Figure 1,2,4,7); (ii) Mapped trimmed reads to genomic regions spanning annotated miRNA *s*⁴⁰ (± 20 nts) and tRNA sequences (± 40 nts) using Bowtie 0.12.7⁴¹ allowing for no mismatches. Next, reads that did not map



without mismatches were aligned to the same regions using SHRIMP2.2.2⁴². SHRIMP2.2.2 seeds were set based on the length of the read allowing 1 mismatch anywhere in the body and up to 3 mismatches at the 3' end of the read (based on the length of the read). (Figure 1a right, Figure 2b, Supplemental Figure 7, Supplemental Table 4). Small RNA-sequencing data was deposited on GEO (GSE57381).

AGO2-RNA Co-immunoprecipitation. FT3-7 cells were grown in Dulbecco's modified Eagle's medium (DMEM, Life Technologies) and supplemented with 10% fetal calf serum and 2 mM GlutaMAX (Life Technologies, Carlsbad, CA). Cells were cultured in a humidified incubator at 37°C and 5% CO₂. Three technical replicates of 1 × 10⁷ FT3-7 cells were harvested in lysis buffer [150 mM KCl, 25 mM Tris-HCl (pH 7.4), 5 mM EDTA, 1% Triton X-100, 5 mM DTT, Complete protease inhibitor mixture (Roche), and 100 U/mL RNaseOUT (Life Technologies)]. Lysates were centrifuged for 30 min at 17,000 × g at 4°C and filtered through a 0.22-um filter. Filtrates were incubated with anti-human AGO2 mAb (RN003M, MBL International, Woborn, MA) or isotype control IgG (Abcam, Cambridge, England) at 4°C for 2 h, followed by addition of 30 μL of Protein G Sepharose (GE Healthcare) for 1 h. The Sepharose beads were washed three times in lysis buffer and RNA extracted using the miRNeasy Mini Kit (Qiagen, Hilden, Germany).

Small RNA real time quantitative PCR (RT-qPCR). Complementary DNA (cDNA) was synthesized using TaqMan MicroRNA Reverse Transcription Kit (Life Technologies) according to the manufacturer's instructions. Real time PCR amplification was performed using TaqMan Universal Master Mix (Life Technologies) on the Bio-Rad CFX96 real time PCR detection system. U6, miR-24, let-7a, let-7f, *RNU48*, and *RNU66* were all evaluated as potential housekeeping small RNAs for purposes of normalization. *RNU48* was selected because it was the most consistent across disease groups. RT-qPCR reactions for human samples were performed in triplicate. RT-qPCR reactions for chimpanzee samples were performed in duplicate. The following TaqMan assays were purchased from Life Technologies: miR-122 (product number 4427975; 002245) and *RNU48* or *SNORD48* (product number 4427975; 001006). Primers for the custom TaqMan assays (5' tRH^{Gly} and 5' tRH^{Val}) were designed using 5'-GCAUUGGUGUAGUGGUAUUCAC-UCUCGCCU-3' for 5' tRH^{Gly} and 5'-GUUCCGUAGUGUAGUGGUAUUCAC-UCUCGCCU-3' for 5' tRH^{Val}.

Metabolic Radiolabeling and Measurement of Nascent Protein Synthesis. Huh7 cells were seeded onto the wells of 6-well cell culture plates at a density of 2 × 10⁵ cells/well and incubated overnight to allow cell attachment. Cells were transfected with 50 nM and 100 nM of 5' tRH^{Gly} (5'-GCAUUGGUGUAGUGGUAUUCAC-UCUCGCCU-3'), 5' tRH^{Val} (5'-GUUCCGUAGUGUAGUGGUAUUCAC-UCUCGCCU-3'), or scramble (5'-GCAUUCACUUGGAUAGAAUCCAAGC-UGAA-3')²¹ (all from Integrated DNA Technologies, Coralville, IA) oligonucleotide after replacing cell culture medium with methionine- and cysteine-deficient DMEM (Life Technologies) and cultured for further 12 hrs. Cells were then metabolically radiolabeled for 12 hrs with 200 μCi/well of Express Protein Labeling Mix containing [³⁵S]methionine and [³⁵S]cysteine (PerkinElmer, Waltham, MA) in the presence or absence of 50 μg/ml puromycin and lysed with lysis buffer (20 mM Tris-HCl [pH 7.4] containing 150 mM NaCl, 1% Triton X-100, 0.05% SDS, and 10% glycerol) supplemented with 50 mM NaF, 5 mM Na₂VO₄, and a protease inhibitor cocktail (Complete; Roche, Mannheim, Germany). The protein concentration of cell lysates was determined by the Bio-Rad Protein Assay (Bio-Rad), and 10 μg (total protein) of cell lysates was subjected to SDS-PAGE followed by staining gels with the Sypro Ruby Protein Gel Stain (Bio-Rad, Hercules, CA) and autoradiography.

Immunohistochemistry (IHC). Staining was performed by immunoperoxidase technique with an Envision kit (DAKO Japan). Primary antibodies used were against β-actin (Cell signaling technology, #4967, Beverly, MA) and Human Angiogenin Affinity Purified Polyclonal Ab (R and D Systems, AF265, Minneapolis, MN).

- Arzumanyan, A., Reis, H. M. & Feitelson, M. A. Pathogenic mechanisms in HBV- and HCV-associated hepatocellular carcinoma. *Nat Rev Cancer* **13**, 123–135 (2013).
- Perz, J. F., Armstrong, G. L., Farrington, L. A., Hutin, Y. J. & Bell, B. P. The contributions of hepatitis B virus and hepatitis C virus infections to cirrhosis and primary liver cancer worldwide. *J Hepatol* **45**, 529–538 (2006).
- Hou, W. & Bonkovsky, H. L. Non-coding RNAs in hepatitis C-induced hepatocellular carcinoma: dysregulation and implications for early detection, diagnosis and therapy. *World J Gastroenterol* **19**, 7836–7845 (2013).
- Xu, X. *et al.* Hepatitis B virus X protein represses miRNA-148a to enhance tumorigenesis. *J Clin Invest* **123**, 630–645 (2013).
- Chen, Y. *et al.* HCV-induced miR-21 contributes to evasion of host immune system by targeting MyD88 and IRAK1. *PLoS Pathog* **9**, e1003248 (2013).
- Jopling, C. L., Yi, M., Lancaster, A. M., Lemon, S. M. & Sarnow, P. Modulation of hepatitis C virus RNA abundance by a liver-specific MicroRNA. *Science* **309**, 1577–1581 (2005).
- Shimakami, T. *et al.* Stabilization of hepatitis C virus RNA by an Ago2-miR-122 complex. *Proc Natl Acad Sci U S A* **109**, 941–946 (2012).
- Janssen, H. L. *et al.* Treatment of HCV Infection by Targeting MicroRNA. *N Engl J Med* **368**, 1685–1694 (2013).
- Garcia-Silva, M. R., Cabrera-Cabrera, F. & Güida, M. C. Hints of tRNA-Derived Small RNAs Role in RNA Silencing Mechanisms. *Genes* **3**, 603–614 (2012).
- Wang, Q. *et al.* Identification and functional characterization of tRNA-derived RNA fragments (tRFs) in respiratory syncytial virus infection. *Mol Ther* **21**, 368–379 (2013).
- Gong, B. *et al.* Compartmentalized, functional role of angiogenin during spotted fever group rickettsia-induced endothelial barrier dysfunction: evidence of possible mediation by host tRNA-derived small noncoding RNAs. *BMC Infect Dis* **13**, 285 (2013).
- Saikia, M. *et al.* Angiogenin-Cleaved tRNA Halves Interact with Cytochrome c Protecting Cells from Apoptosis during Osmotic Stress. *Mol Cell Biol* **34**, 2450–63 (2014).
- Hou, J. *et al.* Identification of miRNomes in human liver and hepatocellular carcinoma reveals miR-199a/b-3p as therapeutic target for hepatocellular carcinoma. *Cancer Cell* **2**, 232–243 (2011).
- Spaniel, C., Honda, M., Selitsky, S. R. & Yamane, D. microRNA-122 abundance in hepatocellular carcinoma and non-tumor liver tissue from Japanese patients with persistent HCV versus HBV infection. *PLoS One* **8**, e76867 (2013).
- Bartel, D. P. MicroRNAs: target recognition and regulatory functions. *Cell* **136**, 215–233 (2009).
- Chan, P. P. & Lowe, T. M. GtRNAdb: a database of transfer RNA genes detected in genomic sequence. *Nucleic Acids Res* **37**, D93–97 (2009).
- Kozomara, A. & Griffiths-Jones, S. miRBase: annotating high confidence microRNAs using deep sequencing data. *Nucleic Acids Res* **42**, D68–73 (2014).
- Lanford, R. E., Lemon, S. M. & Walker, C. in *Hepatitis C Antiviral Drug Discovery & Development* (eds He, Y. & Tan, T.) 99–132 (Horizons Scientific Press, 2011).
- Asabe, S. *et al.* The size of the viral inoculum contributes to the outcome of hepatitis B virus infection. *J Virol* **83**, 9652–9662 (2009).
- Fu, H. *et al.* Stress induces tRNA cleavage by angiogenin in mammalian cells. *FEBS Lett* **583**, 437–442 (2009).
- Yamasaki, S., Ivanov, P., Hu, G.-F. & Anderson, P. Angiogenin cleaves tRNA and promotes stress-induced translational repression. *J Cell Biol* **185**, 35–42 (2009).
- Wang, Q. *et al.* Identification and functional characterization of tRNA-derived RNA fragments (tRFs) in respiratory syncytial virus infection. *Mol Ther* **21**, 368–379 (2013).
- Gong, B. *et al.* Compartmentalized, functional role of angiogenin during spotted fever group rickettsia-induced endothelial barrier dysfunction: evidence of possible mediation by host tRNA-derived small noncoding RNAs. *BMC Infect Dis* **13**, 285 (2013).
- Mishima, E. *et al.* Conformational Change in Transfer RNA Is an Early Indicator of Acute Cellular Damage. *J Am Soc Nephrol* **25**, 2316–26 (2014).
- Ivanov, P., Emara, M. M., Villen, J., Gygi, S. P. & Anderson, P. Angiogenin-induced tRNA fragments inhibit translation initiation. *Mol Cell* **43**, 613–623 (2011).
- Emara, M. M. *et al.* Angiogenin-induced tRNA-derived stress-induced RNAs promote stress-induced stress granule assembly. *J Biol Chem* **285**, 10959–10968 (2010).
- Dhabhi, J. M. *et al.* 5' tRNA halves are present as abundant complexes in serum, concentrated in blood cells, and modulated by aging and calorie restriction. *BMC Genomics* **14**, 298 (2013).
- Vojtech, L. *et al.* Exosomes in human semen carry a distinctive repertoire of small non-coding RNAs with potential regulatory functions. *Nucleic Acids Res* **42**, 7290–7304 (2014).
- Garcia-Silva, M. R. *et al.* Gene Expression Changes Induced by Trypanosoma cruzi Shed Microvesicles in Mammalian Host Cells: Relevance of tRNA-Derived Halves. *Biomed Res Int* **2014**, 305239 (2014).
- Fu, H. *et al.* Stress induces tRNA cleavage by angiogenin in mammalian cells. *FEBS Lett* **583**, 437–442 (2009).
- Yamasaki, S., Ivanov, P., Hu, G.-F. & Anderson, P. Angiogenin cleaves tRNA and promotes stress-induced translational repression. *J Biol Chem* **185**, 35–42 (2009).
- Gao, X. & Xu, Z. Mechanisms of action of angiogenin. *Acta Biochim Biophys Sin (Shanghai)* **40**, 619–624 (2008).
- Pizzo, E. *et al.* Ribonuclease/angiogenin inhibitor 1 regulates stress-induced subcellular localization of angiogenin to control growth and survival. *J Cell Sci* **126**, 4308–4319 (2013).
- Saxena, S. K., Rybak, S. M., Davey, R. T., Youle, R. J. & Ackerman, E. J. Angiogenin is a cytotoxic, tRNA-specific ribonuclease in the RNase A superfamily. *J Biol Chem* **267**, 21982–21986 (1992).
- Mazzanti, R. *et al.* Chronic viral hepatitis induced by hepatitis C but not hepatitis B virus infection correlates with increased liver angiogenesis. *Hepatology* **25**, 229–234 (1997).
- Messerini, L., Novelli, L. & Comin, C. E. Microvessel density and clinicopathological characteristics in hepatitis C virus and hepatitis B virus related hepatocellular carcinoma. *J Clin Pathol* **57**, 867–871 (2004).
- Walker, C. M. Comparative features of hepatitis C virus infection in humans and chimpanzees. *Springer Semin Immunopathol* **19**, 85–98 (1997).
- Mason, W. S. *et al.* Detection of clonally expanded hepatocytes in chimpanzees with chronic hepatitis B virus infection. *J Virol* **83**, 8396–8408 (2009).
- Jackman, J. E. & Alfonzo, J. D. Transfer RNA modifications: nature's combinatorial chemistry playground. *Wiley Interdisciplin Rev RNA* **4**, 35–48 (2013).



40. Kozomara, A. & Griffiths-Jones, S. miRBase: annotating high confidence microRNAs using deep sequencing data. *Nucleic Acids Res* **42**, D68–73 (2014).
41. Langmead, B., Trapnell, C., Pop, M. & Salzberg, S. L. Ultrafast and memory-efficient alignment of short DNA sequences to the human genome. *Genome Biol* **10**, R25 (2009).
42. David, M., Dzamba, M., Lister, D., Ilie, L. & Brudno, M. SHRiMP2: sensitive yet practical short read mapping. *Bioinformatics* **27**, 1011–2 (2011).
43. Larkin, M. A., Blackshields, G., Brown, N. P. & Chenna, R. Clustal W and Clustal X version 2.0. *Bioinformatics* **23**, 2947–2948 (2007).

Acknowledgments

This work was supported by grants from the National Institutes of Health: R00-DK091318 (P.S.); R01-AI095690 and R01-CA164029 (S.M.L.); T32-GM067553 and T32-AI007419 (S.R.S). The Southwest National Primate Research Center is supported by a grant from the NIH Office of Research Infrastructure Programs/OD P51 OD011133), and by Research Facilities Improvement Program Grants C06 RR 12087 and C06 RR016228.

Author contributions

The experiments were designed by S.R.S., P.S. and S.M.L. The data were analyzed by S.R.S.,

J.B., T. Shirasaki, M.H., P.S. and S.M.L. Experiments were performed by S.R.S., D.Y., T.M., E.E.F., B.G. and T. Shirasaki. M.H., T. Shimakami, S.K., R.E.L., S.M.L. and P.S. contributed resources. The manuscript was written by S.R.S., P.S. and S.M.L.

Additional information

Supplementary information accompanies this paper at <http://www.nature.com/scientificreports>

Competing financial interests: The authors declare no competing financial interests.

How to cite this article: Selitsky, S.R. *et al.* Small tRNA-derived RNAs are increased and more abundant than microRNAs in chronic hepatitis B and C. *Sci. Rep.* **5**, 7675; DOI:10.1038/srep07675 (2015).



This work is licensed under a Creative Commons Attribution-NonCommercial-NoDerivs 4.0 International License. The images or other third party material in this article are included in the article's Creative Commons license, unless indicated otherwise in the credit line; if the material is not included under the Creative Commons license, users will need to obtain permission from the license holder in order to reproduce the material. To view a copy of this license, visit <http://creativecommons.org/licenses/by-nc-nd/4.0/>